Nuclear Medicine and Molecular Imaging (2019) 53:396–405
https://doi.org/10.1007/s13139-019-00613-x

ORIGINAL ARTICLE

ISSN (print) 1869-3482
ISSN (online) 1869-3474

Reverse Warburg Effect-Related Mitochondrial Activity and ^{18}F-FDG Uptake in Invasive Ductal Carcinoma

Byung Wook Choi[1] · Young Ju Jeong[2] · Sung Hwan Park[2] · Hoon Kyu Oh[3] · Sungmin Kang[1]

Received: 30 June 2019 / Revised: 23 August 2019 / Accepted: 10 September 2019 / Published online: 28 October 2019

Abstract

Purpose We evaluated the relationship between fluorine-18 fluoro-2-deoxy-glucose (^{18}F-FDG) uptake and mitochondrial activity in cancer cells and investigated the prognostic implications of this relationship in patients with invasive ductal carcinoma of the breast (IDCB).

Methods One hundred forty-six patients with primary IDCB who underwent preoperative ^{18}F-FDG PET/CT followed by curative surgical resection were enrolled in the current study. Mitochondrial activity of cancer cells was assessed based on translocase of outer mitochondrial membrane 20 (TOMM20) expression and cytochrome C oxidase (COX) activity. A Pearson's correlation analysis was used to assess the relationship between the maximum standardized uptake value of the primary tumour (pSUVmax) and mitochondrial activity. Clinicopathological factors, including pSUVmax, histological grade, oestrogen receptor (ER), progesterone receptor (PR), and TOMM20 expression; and COX activity, were assessed for the prediction of disease-free survival (DFS) using the Kaplan–Meier method and Cox proportional hazards model.

Results Fourteen of the 146 subjects (9.6%) showed tumour recurrence. There was a significant positive correlation between ^{18}F-FDG uptake and the mitochondrial activity of cancer cells in patients with IDCB, and increased ^{18}F-FDG uptake and mitochondrial activity were significantly associated with a shorter DFS. Additionally, results from the receiver-operating curve analysis demonstrated that the cut-off values of pSUVmax, TOMM20 expression, and COX activity for the prediction of DFS were 7.76, 4, and 5, respectively. Further, results from the univariate analysis revealed that pSUVmax, TOMM20 expression, PR status, and histologic grade were significantly associated with DFS; however, the multivariate analysis revealed that only pSUVmax was associated with DFS (HR, 6.51; 95% CI, 1.91, 22.20; $P = 0.003$).

Conclusions The assessment of preoperative ^{18}F-FDG uptake and post-surgical mitochondrial activity may be used for the prediction of DFS in patients with IDCB.

Keywords ^{18}F-FDG · Breast cancer · Cytochrome c oxidase · Invasive ductal carcinoma · Reverse Warburg effect · Translocase of outer mitochondrial membrane 20

Introduction

Breast cancer is one of the most frequently diagnosed cancers worldwide and is a leading cause of cancer-related deaths in women. In the USA, approximately 271,270 new cases of breast cancer will be diagnosed and 42,260 deaths will occur in 2019 [1]. Invasive ductal carcinoma (IDC) is the most common form of breast cancer and accounts for 55% of diagnosed breast cancer cases [2]. Additionally, because breast cancer presents a wide range of biological heterogeneity, its prognosis, recurrence patterns, and responses to primary treatments are highly variable. Therefore, understanding the biology of

✉ Sungmin Kang
kufa77@naver.com

[1] Department of Nuclear Medicine, Catholic University of Daegu School of Medicine, 33, Duryugongwon-ro 17-gil, Nam-gu, Daegu 42472, Republic of Korea

[2] Department of Surgery, Catholic University of Daegu School of Medicine, Daegu, Republic of Korea

[3] Department of Pathology, Catholic University of Daegu School of Medicine, Daegu, Republic of Korea

breast cancer may help establish a more appropriate treatment strategy and improve the prognosis of affected individuals.

Under normal conditions, cells in the human body primarily produce energy via mitochondrial oxidative phosphorylation (OXPHOS); however, despite the aerobic environment, cancer cells preferentially use glycolysis, which is less efficient than OXPHOS and generates less adenosine triphosphate (ATP) per molecule of glucose than the OXPHOS pathway generates [3, 4]. This concept was first presented by Otto H. Warburg in the 1920s and is referred to as aerobic glycolysis; anaerobic glycolysis had already been defined as the conversion of glucose to L-lactate under oxygen-poor conditions [5]. This phenomenon was later termed "the Warburg effect" and has been observed in a variety of cancers, including breast and colorectal cancer [6, 7]. Warburg later hypothesised that mitochondrial dysfunction caused by irreversible mitochondrial damage underlies aerobic glycolysis [8], and this altered glycolytic feature of cancer cells is the basis of fluorine-18 fluoro-2-deoxy-glucose positron emission tomography/computed tomography (^{18}F-FDG PET/CT) [3]. Although the Warburg effect is not applicable to all human cancers, it is a widely accepted concept that is used to understand tumour metabolism.

Recently, a new concept, termed the "reverse Warburg effect," was proposed to understand cancer metabolism in more detail [9–12]. According to the reverse Warburg effect, cancer cells induce oxidative stress in neighbouring stromal cancer-associated fibroblasts (CAFs). This oxidative stress induces the Warburg effect in CAFs that subsequently secrete high energy metabolites, such as pyruvate and L-lactate (from aerobic glycolysis). Cancer cells then take up these metabolites and use them in the mitochondrial tricarboxylic acid (TCA) cycle and OXPHOS [9, 10]. Indeed, studies have demonstrated that cancer cells metabolically parasitize the adjacent CAFs in some types of human tumours, including breast cancer [9–12].

^{18}F-FDG PET/CT is a well-established imaging modality that has been widely used for staging, restaging, treatment-response assessment, and the prediction of prognosis in breast cancer [13]. Additionally, ^{18}F-FDG PET/CT reflects the glucose metabolism of cancer cells; therefore, ^{18}F-FDG uptake in primary tumours is strongly correlated with the increased mitochondrial activity of cancer cells, and this is represented by sustained OXPHOS of the cancer cells and active aerobic glycolysis of CAFs [12, 14]. The presence of functional mitochondrial activity can be recognized by immunohistochemical (IHC) staining of the translocase of outer mitochondrial membrane 20 (TOMM20) and cytochrome C oxidase (COX) [4, 15]. However, the relationship between ^{18}F-FDG uptake and mitochondrial activity in IDC of the breast (IDCB) has not been completely elucidated, and only a few studies have reported findings regarding the prognostic value of mitochondrial activity in IDCB [16–18].

Therefore, the purpose of this retrospective study was to investigate the relationship between ^{18}F-FDG uptake and mitochondrial activity and to evaluate the prognostic value of this relationship in patients with IDCB.

Materials and Methods

Study Subjects

In this retrospective study, we reviewed the medical records of patients with IDCB who underwent preoperative ^{18}F-FDG PET/CT followed by curative surgical resection from the healthcare information system between July 2010 and December 2015. Patients who were diagnosed with primary IDCB using postoperative histopathological examination of resected tissue were included in this study. Patients who were diagnosed with excisional biopsy or who received neoadjuvant chemotherapy and patients with other pathologies, such as lobular carcinoma or lymphoma, synchronous bilateral breast cancer, a history of other primary malignancy, recurrent cancer, or distant metastasis were excluded from participation. Finally, a total of 146 patients were enrolled in the current study. This study was approved by the institutional review board at our institution (CR-15-052), and the need to obtain written informed patient consent was waived due to the retrospective design of this study.

^{18}F-FDG PET/CT Acquisition

All patients fasted for at least 6 h before ^{18}F-FDG injections, and patients' blood glucose levels were confirmed to be < 150 mg/dl. A dose of 7.0 MBq/kg of ^{18}F-FDG was administered intravenously, and patients were encouraged to rest for 60 min before acquisition of the PET/CT image. ^{18}F-FDG PET/CT scans were performed using an integrated PET/CT system (Discovery STE; GE Healthcare, Milwaukee, WI, USA). A low-dose non-contrast CT scan was performed for attenuation correction. Immediately following the CT scan, standard PET imaging was performed from the base of the skull to the proximal thigh with an acquisition time of 3 min per bed position in the 3D mode. PET images were reconstructed using an ordered-subset expectation maximization algorithm with the low-dose CT data sets. PET images were then fused with CT images.

Image Analysis

All ^{18}F-FDG PET/CT images were retrospectively reviewed on a vendor-supplied dedicated workstation (GE Advantage Workstation version 4.7, GE Healthcare). Two experienced nuclear medicine physicians interpreted ^{18}F-FDG PET/CT images of all patients until a consensus was met. An

ellipsoidal volume of interest (VOI) was manually drawn to encompass the primary breast cancer lesion on the fused PET/CT images, and the maximum standardized uptake value (SUVmax) was measured from the VOI based on body weight. The SUVmax was recorded and presented as the pSUVmax.

Investigation of Histological Parameters

We assessed the expression of hormone receptors, including the oestrogen receptor (ER), progesterone receptor (PR), and human epidermal growth factor receptor 2 (HER2), after surgery using the pathological reports derived from the healthcare information system. Additionally, we investigated the expression of TOMM20 and COX activity according to the following procedures.

(1). Construction of Tissue Microarrays

The preparation of tissue microarray (TMA) production was performed in accordance with published protocols [19, 20]. First, the donor blocks of breast cancer tissue were prepared to produce haematoxylin and eosin (H&E)-stained microscopic slides. Then, relevant paraffin tumour blocks were chosen according to the evaluation of slides by an experienced pathologist. A TMA instrument (Quick-Ray™ manual punch arrayer; Uni-Tech Science, Seoul, South Korea) was used to acquire two tumour tissue cores with a 2-mm diameter from each of the donor blocks. The cores were placed into a recipient block that contained 46 tissue cores. A total of 18 TMA blocks containing both tumour and control tissue samples were used in this study. Multiple sections (5-μm in thickness) were cut from the TMA blocks to generate TMA slides using a microtome. Finally, the TMA slides were reviewed under a light microscope to identify the presence of relevant tumour areas.

(2). Immunohistochemical Staining and Interpretation

We investigated the expression of TOMM20 and COX activity using IHC staining as previously described [20]. Briefly, IHC staining was performed on 5-μm-thick TMA tissue sections using the Bond Polymer Intense Detection System (Leica Microsystems, Nusslock, Germany). Tissue sections were deparaffinized with Bond Dewax Solution (Leica Microsystems) and rehydrated with decreasing concentrations of ethanol in water. Additionally, an antigen retrieval was achieved using Bond ER Solution (Leica Microsystems) for 30 min at 100 °C. Endogenous peroxidases were quenched by incubating the slides in hydrogen peroxide for 5 min. The slides were incubated for 15 min at room temperature with monoclonal antibodies against TOMM20 (1:500, polyclonal, GTX32928, GeneTex, Irvine, CA, USA) and COX (1:700, monoclonal, GTX628886, GeneTex). These antibodies are available in our hospital using a biotin-free polymeric horseradish peroxidase-linker antibody conjugate system in a Bond-Max automatic slide stainer (Leica Microsystems). The TOMM20 and COX expression was scored according to the intensity of staining in tumour cells and the proportion of cells exhibiting cytoplasmic staining according to modifications of the Allred scoring system (Fig.1) [21].

Clinical Recurrence Assessment

All patients underwent surgical resection with a curative purpose, and patients received postoperative adjuvant chemotherapy, radiotherapy, and hormonal therapy according to tumour status or the medical condition of each patient. During the follow-up period, physical examination, tumour markers on laboratory tests, mammography, and breast ultrasonography (USG) were performed as part of the routine follow-up protocol. Recurrence was defined as newly diagnosed locoregional recurrence or distant metastasis on imaging studies. When recurrence of the disease was suspected during the follow-up period, breast magnetic resonance image or chest CT, whole body bone scan, and ^{18}F-FDG PET/CT were used for the diagnosis of the disease, and/or suspicious lesions were histologically confirmed by fine-needle aspiration cytology or biopsy. Disease-free survival (DFS) was used to evaluate the predictive ability of pSUVmax and histologic parameters. DFS was defined as the number of months from the date of curative surgery to the date of the first recurrence.

Statistical Analysis

Descriptive statistical values are expressed as the mean ± standard deviation (SD). The clinicopathological variables that were used for comparisons and survival analyses were pSUVmax; age; cancer stage; pathologic T stage; presence of lymph node metastasis; histological grade of the primary tumour; ER, PR, HER2, and TOMM20 expression; and COX activity. A Pearson's correlation analysis was conducted to evaluate the associations between pSUVmax and TOMM20 expression, pSUVmax and COX activity, and TOMM20 expression and COX activity. Comparisons of pSUVmax values according to clinicopathological parameters were evaluated using the independent *t* test, Mann–Whitney *U* test, Kruskal–Wallis test, and one-way analysis of variance (ANOVA). For survival analysis, continuous variables of pSUVmax, TOMM20 expression, and COX activity were dichotomized using an optimal cut-off value by receiver-operating characteristic (ROC) curve analysis. A Kaplan–Meier analysis with a log-rank test was performed for univariate survival analysis. Significant variables ($P < 0.1$) from the univariate analysis were entered into a multivariate analysis

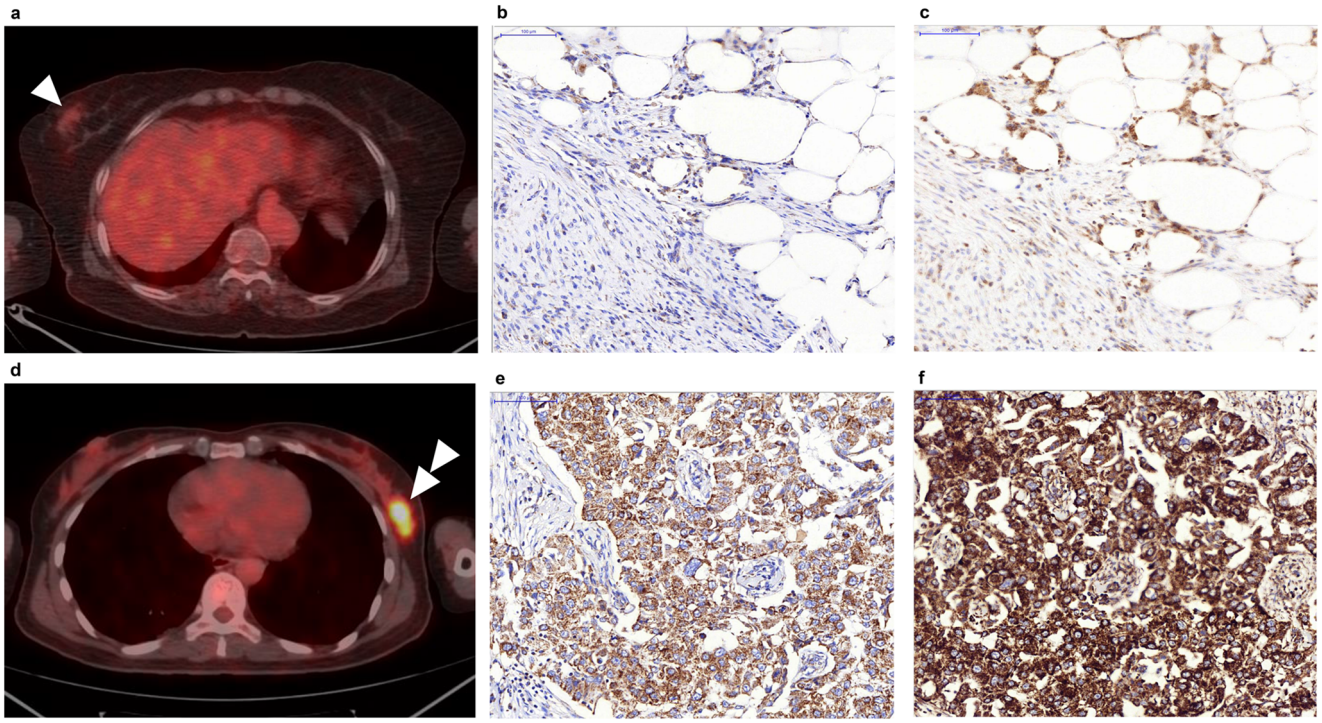

Fig. 1 ^{18}F-FDG PET/CT and TOMM20 and COX expression of representative cases. **a**–**c** A 74-year-old female patient with right IDCB and no regional lymph node metastasis: **a** The preoperative transverse fusion PET-CT image revealed a relatively low SUVmax of 1.96 at the primary mass (arrow head). Stromal immunohistochemical staining (brown colour) of the primary tumour: **b** TOMM20 score, 2 (proportion score [PS] 1 + intensity score [IS] 1) and **c** COX score, 3 (PS1 + IS 2). The patient received curative surgery and hormonal therapy, and she survived for 50.6 months without recurrence. **d**–**f** A 40-year-old female patient with left IDCB and axillary lymph node metastasis: **d** Transverse fusion image of PET/CT revealed a relatively high SUVmax of 10.12 at the primary tumour (double arrow heads). **e** TOMM20 score, 7 (PS5 + IS 2), and **f** COX score, 8 (PS5 + IS3). The patient received curative resection following adjuvant chemotherapy and hormonal therapy. Distant metastasis in both lungs were noted at 22 months after initial treatment. (× 400). ^{18}F-FDG PET/CT, fluorine-18 fluoro-2-deoxy-glucose positron emission tomography/computed tomography; TOMM20, translocase of outer mitochondrial membrane 20; COX, cytochrome C oxidase; IDCB, invasive ductal carcinoma of the breast; SUVmax, maximum standardized uptake value; PS, proportion score; IS, intensity score

that was performed using a multivariable Cox proportional hazard model.

All statistical analyses were performed using MedCalc version 18.11.6 for Windows (MedCalc software bvba, Ostend, Belgium), and $P < 0.05$ indicated statistical significance.

Results

Patient Characteristics

One-hundred-and-forty-six patients with IDCB were enrolled in this study. Clinicopathological characteristics of patients are presented in Table 1. The mean age of patients was 53.9 ± 11.6 years (range 33–90 years), the median follow-up period was 56.1 months (mean ± SD = 51.9 ± 19.9, range 1.0–97.2 months), and the TNM stage was classified according to the American Committee on Cancer (AJCC) Cancer Staging Manual 7th edition. The primary tumour stages (T) (according to size) were as follows: T stage 1a/b, 31 patients (21.2%); T stage 1c, 62 patients (42.5%); and T stage 2, 53 patients (36.3%). Pathologically confirmed axillary lymph node (LN) involvement was observed in 60 patients (61.1%), and 64 (43.8%), 64 (43.8%), and 18 (12.3%) patients were classified as stage I, stage II, and stage III, respectively. All patients received adjuvant chemotherapy ($n = 118$), radiotherapy ($n = 84$), and hormonal therapy ($n = 108$) according to clinical status. Two patients did not receive adjuvant treatment, 14 patients received chemotherapy only, 13 patients received hormonal therapy only, and 3 patients received radiotherapy only. Thirty-three patients received chemotherapy and hormonal therapy, 19 patients received chemotherapy and radiotherapy, and 10 patients received hormonal and radiotherapy. The remaining 52 patients received chemotherapy, hormonal therapy, and radiotherapy. Among the 146 patients, 132 (90.4%) patients were disease-free, and tumour recurrence was observed in 14 (9.6%) patients during the follow-up period. The median follow-up time to recurrence was 24.0 months (mean ± SD: 26.3 ± 12.1 months, range 11.7–55.0 months). Among patients with recurrence, 4 patients showed cancer-related death.

Table 1 Patient characteristics

Characteristics	Value
Number of patients	146
Age, median (range)	53.9 (33–90)
Follow-up time (months, mean ± SD)	51.9 ± 19.9
Pathological tumour size*	
T1a/b	31 (21.2%)
T1/c	62 (42.5%)
T2	53 (36.3%)
Histologic grade of tumour	
Grade 1	36 (24.7%)
Grade 2	51 (34.9%)
Grade 3	59 (40.4%)
Axillary lymph node involvement	
Negative	86 (58.9%)
Positive	60 (41.1%)
Stage, pathologic*	
I	64 (43.8%)
II	64 (43.8%)
III	18 (12.3%)
ER	
Positive	105 (71.9%)
Negative	41 (28.1%)
PR	
Positive	111 (76.0%)
Negative	35 (24.0%)
HER2	
Positive	119 (81.5%)
Negative	27 (18.5%)
Recurrence	
No	132 (90.4%)
Yes	14 (9.6%)

* According to the American Joint Committee on Cancer (AJCC) 7th edition, *SD*, standard deviation; *ER*, oestrogen receptor; *PR*, progesterone receptor; *HER2*, human epidermal growth factor 2

Relationship between pSUVmax and Indexes of Mitochondrial Activity

The Pearson's correlation analysis demonstrated that there was a significant positive correlation between pSUVmax and TOMM20 expression ($r = 0.349$, $P < 0.001$), pSUVmax and COX activity ($r = 0.384$, $P < 0.001$), and TOMM20 expression and COX activity ($r = 0.832$, $P < 0.001$). The optimal cut-off values for categorizing low and high pSUVmax, TOMM20 expression, and COX activity for the prediction of tumour recurrence using the ROC curve analysis were 7.76, 4, and 5, respectively (Table 2 and Fig. 2). Patients were dichotomized according to each optimal cut-off value.

Table 2 ROC analysis to determine optimal cut-off values of parameters

Parameters	Optimal cut-off value	AUC (95% CI)	*P* value
pSUVmax	7.76	0.736 (0.226–0.665)	0.003
TOMM20	4	0.622 (0.227–0.409)	0.043
COX	5	0.642 (0.083–0.312)	0.033

AUC, area under curve; *CI* confidence interval; *pSUVmax*, maximum standardized uptake value of the primary tumour; *TOMM20*, translocase of outer mitochondrial membrane 20; *COX*, cytochrome C oxidase

Comparisons of pSUVmax Values According to Clinicopathological Parameters

Difference in pSUVmax were obtained according to the clinicopathological parameters. The mean pSUVmax of the 146 patients was 4.5 ± 3.7 (range, 0.7 to 18.7). The mean pSUVmax in the high TOMM20 expression (> 4) and high COX activity (> 5) groups was significantly higher than that in the low TOMM20 expression (≤ 4) and low COX activity (≤ 5) groups ($P < 0.001$, respectively). The mean pSUVmax in the disease-free group (4.2 ± 3.5) was significantly lower than that in the relapse group (7.5 ± 4.4; $P = 0.004$). The mean pSUVmax was significantly higher in ER-negative tumours ($P = 0.004$), PR-negative tumours ($P = 0.030$), and in tumours with LN metastasis ($P = 0.038$) than that in ER-positive

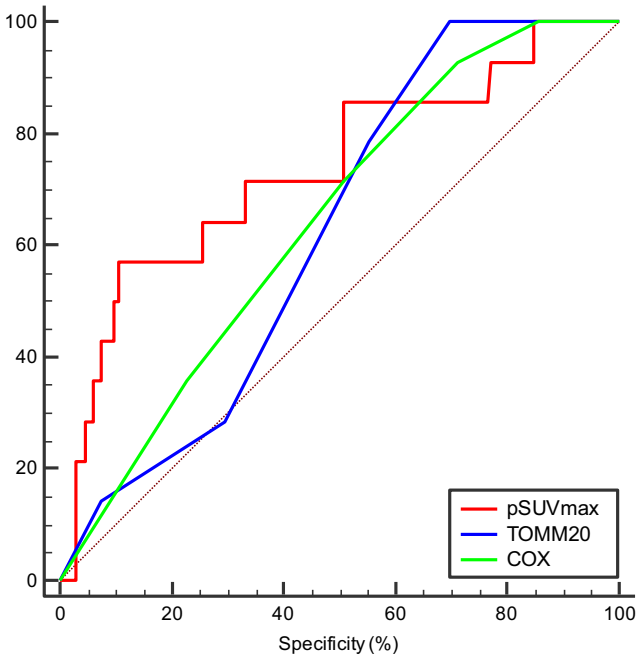

Fig. 2 Receiver-operating characteristic curve analysis for the prediction of tumour recurrence using pSUVmax, TOMM20 expression, and COX activity. The pSUVmax had the greatest AUC (0.736; 95% confidence interval, 0.226 to 0.665) as compared with the AUC of other parameters. pSUVmax, maximum standard uptake value of the primary tumour; TOMM20, translocase of outer mitochondrial membrane 20; COX, cytochrome C oxidase; AUC, are under the curve

tumours, PR-negative tumours, and tumours without LN metastasis, respectively. There was no significant difference in the mean pSUVmax according to HER2 status ($P = 0.459$). Comparisons of the mean pSUVmax values according to the histological grade of the primary tumour revealed that the mean pSUVmax of histological grade 3 tumours was significantly higher than that of histological grades 1 and 2 tumours ($P < 0.001$, respectively); there was no significant difference in the mean pSUVmax between histological grade 1 and 2 tumours. There was a significant difference in the pSUVmax according to the T stage groups ($P < 0.001$). Specifically, a post-hoc analysis with Bonferroni correction demonstrated that the mean pSUVmax was significantly higher in the order of T2 (6.7 ± 4.3), T1c (3.8 ± 2.8), and T1a/b (2.0 ± 0.8) groups. Additionally, the mean pSUVmax of patients in the stage I group (3.0 ± 2.5) was significantly lower than that of patients in the stage II (5.7 ± 4.2) and stage III (5.6 ± 3.3) groups (stage I vs II, $P < 0.001$; I vs III, $P = 0.001$), but the post-hoc analysis revealed that the mean pSUVmax between the stage II and III groups was not significantly different ($P = 0.858$).

Prognostic Evaluation of pSUVmax and Histological Parameters

We performed a Kaplan-Meier survival analysis for the prediction of DFS with pSUVmax and histological factors, including TOMM20 expression; COX activity; ER, PR, and HER2 status; and histologic grade. The univariate analysis revealed that pSUVmax, TOMM20 expression, PR status, and histologic grade were significantly associated with DFS. However, COX activity, ER, and HER2 status were not significantly associated with DFS (Fig. 3). The multivariate analysis was performed using the Cox proportional hazards regression analysis and included pSUVmax, TOMM20 expression, PR status, and histological grade. However, this analysis showed that the pSUVmax was the only factor that was significantly associated with a decreased DFS (HR, 5.85; 95% CI, 1.72, 19.91; $P = 0.005$). Other histological parameters, including TOMM20 expression, PR status, and histological grade were not associated with DFS according to the results of the multivariate analysis (Table 3).

Discussion

To the best of our knowledge, previous studies have not investigated the relationship between ^{18}F-FDG uptake and mitochondrial activity (represented by TOMM20 expression and COX activity) in the tumour mass and the prognostic implications of this relationship in patients with IDCB. Our findings demonstrated that mitochondrial activity in the primary mass of IDCB was significantly positively correlated with

Fig. 3 Kaplan–Meier analysis of disease-free survival according to pSUVmax and other histological parameters. Fourteen of the 146 subjects experienced tumour recurrence during the follow-up period. **a** pSUVmax, **b** TOMM20, **c** COX, **d** ER, **e** PR, **f** HER2, and **g** histologic grade. pSUVmax, maximum standard uptake value of the primary tumour; TOMM20, translocase of outer mitochondrial membrane 20; COX, cytochrome C oxidase; ER, oestrogen receptor; PR, progesterone receptor; HER2, human epidermal growth factor 2

^{18}F-FDG uptake. Additionally, increased ^{18}F-FDG uptake and expression of TOMM20 in the primary IDCB mass were significantly associated with poor DFS. These results support the reverse Warburg effect that sustains OXPHOS in cancer cells and increases aerobic glycolysis of CAFs. Moreover, increased pSUVmax and increased mitochondrial activity may be used as prognostic indicators for predicting DFS.

The Warburg effect mainly focuses on metabolism in cancer cells. Therefore, this may partially explain tumour metabolism; there are very reports on metabolic interactions between cancer cells and the adjacent tumour microenvironment (TME) [22–24]. In contrast to the Warburg effect, the reverse Warburg effect, also known as the two-compartment model, considers interactions between cancer cells and the TME, particularly CAFs [9, 10, 15, 25]. In this model, cancer cells trigger the production of reactive oxygen species in neighbouring CAFs by secreting hydrogen peroxide into the TME. Then, oxidative stress causes a decrease in mitochondrial activity and an increase in glucose uptake that supports aerobic glycolysis in CAFs. Consequently, the CAFs produce high energy metabolites (such as L-lactate, pyruvate, ketone bodies, and glutamine) and release these mitochondrial fuels into the TME. The release of these fuels subsequently causes stimulation of OXPHOS in cancer cells. Thereafter, these energy-rich mitochondrial fuels are taken up by cancer cells, and this allows for the efficient production of ATP via mitochondrial OXPHOS [10, 26].

Previous studies have demonstrated that cancer cells exhibit increased mitochondrial activity in some types of human cancers, such as breast, colorectal, lymphoma, lung, and head and neck cancers [4, 9–12, 17, 18, 25, 27–29]. In these studies, several biomarkers, including monocarboxylate transporter 1 (MCT1), MCT4, TOMM20, and COX, have been proposed for the identification of tumour metabolism using OXPHOS. Additionally, studies have reported that MCT1 and MCT4 play an important role in the relationship between cancer cells and CAFs. For example, MCT1 mediates the influx of lactate into cells and has been found to be upregulated in cancer cells with sustained OXPHOS, and MCT4 mediates the efflux of lactate from cells and has been found to be upregulated in CAFs [30–33]. Therefore, energy-rich fuels, such as L-lactate, are generated in CAFs using aerobic glycolysis and are secreted via MCT4. Then, these energy-rich fuels are taken up into cancer cells via MCT1 and are utilized for the efficient production of ATP via mitochondrial OXPHOS [25, 31]. Several

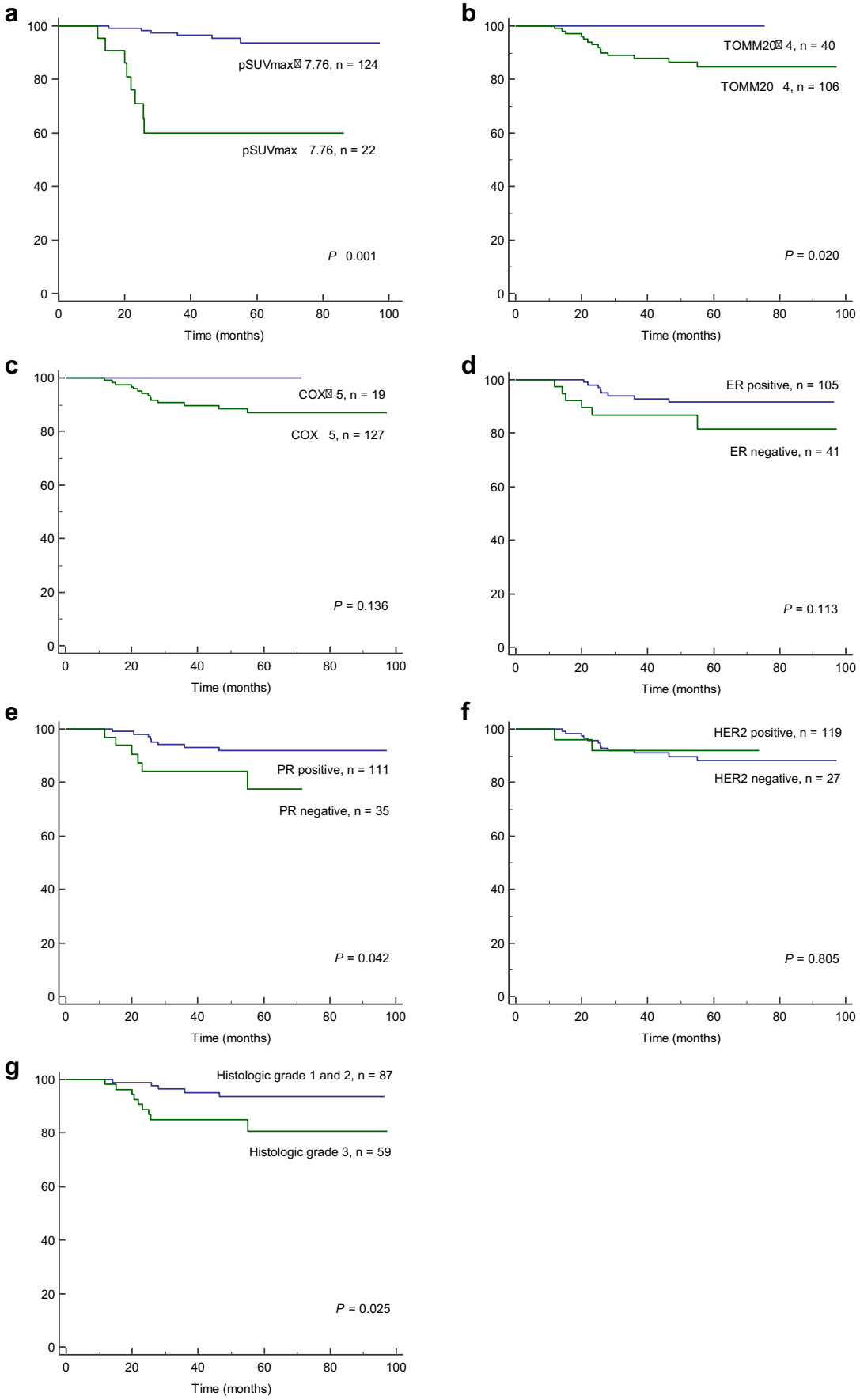
a
pSUVmax 7.76, n = 124
pSUVmax 7.76, n = 22
P 0.001
Time (months)
b
TOMM20 4, n = 40
TOMM20 4, n = 106
P = 0.020
Time (months)
c
COX 5, n = 19
COX 5, n = 127
P = 0.136
Time (months)
d
ER positive, n = 105
ER negative, n = 41
P = 0.113
Time (months)
e
PR positive, n = 111
PR negative, n = 35
P = 0.042
Time (months)
f
HER2 positive, n = 119
HER2 negative, n = 27
P = 0.805
Time (months)
g
Histologic grade 1 and 2, n = 87
Histologic grade 3, n = 59
P = 0.025
Time (months)

Table 3 Parameters for predicting disease-free survival using the Cox proportional hazard regression model

Parameters	HR (95% CI)	*P* value
pSUVmax (> 7.76 vs. ≤ 7.76)	5.85 (1.72, 19.91)	0.005*
TOMM20 (> 4 vs. ≤ 4)	5.48E + 05 (1.25E-232, 2.40E + 243)	0.962
PR (positive vs. negative)	1.32 (0.41, 4.27)	0.647
Histologic grade of primary tumour (1, 2 vs. 3)	1.17 (0.45, 3.04)	0.753

*Statistically significant, *HR* hazard ratio; *CI*, confidence interval; *pSUVmax*, maximum standardized uptake value of the primary tumour; *TOMM20*, translocase of outer mitochondrial membrane 20; *PR*, progesterone receptor

studies have also evaluated the relationship between MCT expression and patient outcomes [4, 16–18, 34]. In these studies, the high expression of MCT1 and MCT4 was significantly associated with shorter PFS or overall survival. TOMM20 is a receptor subunit of the mitochondrial membrane import pore, and COX is the terminal enzyme in the mitochondrial electron transport chain [35, 36]. Therefore, the increased expression and activity of these markers in cancer cells provide evidence of active mitochondria and OXPHOS metabolism. Curry et al. [4] reported that there was a strong positive expression of TOMM20 and COX activity in poorly differentiated cancer cells in head and neck squamous cell cancer [4], and similar results were observed in the current study. Specifically, TOMM20 expression and COX activity were significantly higher in histological grade 3 primary IDCB tumour masses than TOMM20 expression and COX activity in histological grade 1/2 masses (data not shown). Additionally, TOMM20 expression was significantly associated with a shorter DFS.

Increased ^{18}F-FDG uptake in the primary IDCB tumour mass was originally thought to be entirely due to cancer cells via the Warburg effect. However, the concept of the reverse Warburg effect has generated a change in the understanding of ^{18}F-FDG uptake in the primary tumour mass on ^{18}F-FDG PET/CT. According to the reverse Warburg effect, increased glucose uptake is expected in cancer cells and CAFs. Martinez-Outschoorn et al. [10] reported that the glucose uptake levels of fibroblasts and cancer cells were relatively similar under single-cell culture conditions. However, glucose uptake in fibroblasts was increased 3-fold as compared with glucose uptake in cancer cells under identical co-culture conditions [10]. Therefore, the level of ^{18}F-FDG uptake in the primary tumour mass may more accurately represent the glucose metabolism of CAFs than that of cancer cells. Although there was a significant positive correlation between pSUVmax and mitochondrial activity in the current study, the correlation coefficient was moderate. This may be explained by differences between the ^{18}F-FDG uptake ratio of breast cancer cells and neighbouring CAFs and the ^{18}F-FDG uptake ratio of the cells that were used in the laboratory co-culture conditions. Further studies with parameters that represent glycolysis in cancer cells and CAFs are needed to understand glucose metabolism in IDCB.

Several studies have demonstrated that ^{18}F-FDG uptake in IDCB, which is presented as pSUVmax, is significantly associated with histopathological and immunochemical factors, such as ER, PR, and HER2 expression, and histological grade [37–39]. Additionally, preoperative pSUVmax is a significant prognostic factor in primary breast cancer [38, 40–43]. In the current study, similar results were found. Specifically, PR-negativity, high histological grade, high pSUVmax, and increased TOMM20 expression were significantly associated with shorter DFS in our univariate analysis. Further, high pSUVmax was the only risk factor that predicted recurrence in the multivariate analysis. Similarly, previous studies have demonstrated that sustained OXPHOS and active aerobic glycolysis in breast cancer cells and CAFs, which represent an active reverse Warburg effect, were significantly associated with poor prognosis [16–18]. Thus, ^{18}F-FDG PET/CT may be a useful modality for visualizing the reverse Warburg effect and may be a surrogate marker of a lethal TME in patients with IDCB. ^{18}F-FDG PET/CT may also be used to facilitate the establishment of a treatment strategy via visualization of tumoral heterogeneity and to identify treatment responses to chemotherapy targeting mitochondrial metabolism [44].

There were several limitations of the current study. First, this was a retrospective, single centre study with a relatively small sample size, and these issues may have increased the risk of selection bias. Further studies with a larger number of patients are needed to validate the results of the present study. Additionally, we did not investigate the relationship between pSUVmax and other markers of mitochondrial metabolism, such as MCT1 or MCT4. However, we showed a positive correlation between pSUVmax and sustained mitochondrial activity in cancer cells, and this correlation may explain the reverse Warburg effect in IDCB and act as a substitute for other markers. Nevertheless, additional prospectively designed studies that focus on the relationship between ^{18}F-FDG PET and known markers of mitochondrial metabolism are required to gain a better understanding of tumour

metabolism and its prognostic implications. Further, the T stage of more than half of the patients in this study was below T1. This may have resulted in an underestimation of the pSUVmax because we did not correct for the partial volume effect. An appropriate partial volume effect-correction method would facilitate the precise measurement of pSUVmax, even in early T stage tumours. Finally, we did not perform histopathological confirmation in a few subjects who showed recurrence; however, this practice may not be appropriate for all cases in the clinical practice, particularly in cases of suspected bone metastasis.

Conclusion

In conclusion, our study findings provide insights into cancer glucose metabolism and support for the reverse Warburg effect. We observed a significant positive correlation between ^{18}F-FDG uptake and mitochondrial activity in patients with IDCB. These findings represent sustained mitochondrial OXPHOS in cancer cells and increased aerobic glycolysis in CAFs. Moreover, increased ^{18}F-FDG uptake and mitochondrial activity were significantly associated with a shorter DFS. Therefore, investigations of preoperative ^{18}F-FDG uptake and post-surgical mitochondrial activity in patients with IDCB may be used as markers for the prediction of DFS.

Compliance with Ethical Standards

Conflict of Interest Byung Wook Choi, Young Ju Jeong, Sung Hwan Park, Hoon Kyu Oh, and Sungmin Kang declare that they have no conflict of interest.

Ethical Approval All procedures performed in studies involving human participants were in accordance with the ethical standards of the institutional and/or national research committee and with the 1964 Helsinki Declaration and its later amendments or comparable ethical standards. For this type of study, formal consent is not required.

Informed Consent The institutional review board of our institute approved this retrospective study, and the requirement to obtain informed consent was waived.

References

1. Siegel RL, Miller KD, Jemal A. Cancer statistics, 2019. CA Cancer J Clin. 2019;69:7–34.
2. Eheman CR, Shaw KM, Ryerson AB, Miller JW, Ajani UA, White MC. The changing incidence of in situ and invasive ductal and lobular breast carcinomas: United States, 1999-2004. Cancer Epidemiol Biomark Prev. 2009;18:1763–9.
3. Vander Heiden MG, Cantley LC, Thompson CB. Understanding the Warburg effect: the metabolic requirements of cell proliferation. Science. 2009;324:1029–33.
4. Curry JM, Tuluc M, Whitaker-Menezes D, Ames JA, Anantharaman A, Butera A, et al. Cancer metabolism, stemness and tumor recurrence: MCT1 and MCT4 are functional biomarkers of metabolic symbiosis in head and neck cancer. Cell Cycle. 2013;12:1371–84.
5. Warburg O. The metabolism of carcinoma cells. Cancer Res. 1925;9:148–63.
6. Grover-McKay M, Walsh SA, Seftor EA, Thomas PA, Hendrix MJ. Role for glucose transporter 1 protein in human breast cancer. Pathol Oncol Res. 1998;4:115–20.
7. Fang S, Fang X. Advances in glucose metabolism research in colorectal cancer. Biomed Rep. 2016;5:289–95.
8. Warburg O. On the origin of cancer cells. Science. 1956;123:309–14.
9. Pavlides S, Whitaker-Menezes D, Castello-Cros R, Flomenberg N, Witkiewicz AK, Frank PG, et al. The reverse Warburg effect: aerobic glycolysis in cancer associated fibroblasts and the tumor stroma. Cell Cycle. 2009;8:3984–4001.
10. Martinez-Outschoorn UE, Lin Z, Trimmer C, Flomenberg N, Wang C, Pavlides S, et al. Cancer cells metabolically "fertilize" the tumor microenvironment with hydrogen peroxide, driving the Warburg effect: implications for PET imaging of human tumors. Cell Cycle. 2011;10:2504–20.
11. Huebbers CU, Adam AC, Preuss SF, Schiffer T, Schilder S, Guntinas-Lichius O, et al. High glucose uptake unexpectedly is accompanied by high levels of the mitochondrial ß-F1-ATPase subunit in head and neck squamous cell carcinoma. Oncotarget. 2015;6:36172–84.
12. Koit A, Shevchuk I, Ounpuu L, Klepinin A, Chekulayev V, Timohhina N, et al. Mitochondrial respiration in human colorectal and breast cancer clinical material is regulated differently. Oxidative Med Cell Longev. 2017;2017:1372640.
13. Caresia Aroztegui AP, García Vicente AM, Alvarez Ruiz S, Delgado Bolton RC, Orcajo Rincon J, Garcia Garzon JR, et al. 18F-FDG PET/CT in breast cancer: evidence-based recommendations in initial staging. Tumour Biol. 2017;39:1010428317728285.
14. Kaambre T, Chekulayev V, Shevchuk I, Karu-Varikmaa M, Timohhina N, Tepp K, et al. Metabolic control analysis of cellular respiration in situ in intraoperational samples of human breast cancer. J Bioenerg Biomembr. 2012;44:539–58.
15. Whitaker-Menezes D, Martinez-Outschoorn UE, Flomenberg N, Birbe RC, Witkiewicz AK, Howell A, et al. Hyperactivation of oxidative mitochondrial metabolism in epithelial cancer cells in situ: visualizing the therapeutic effects of metformin in tumor tissue. Cell Cycle. 2011;10:4047–64.
16. Sotgia F, Martinez-Outschoorn UE, Pavlides S, Howell A, Pestell RG, Lisanti MP. Understanding the Warburg effect and the prognostic value of stromal caveolin-1 as a marker of a lethal tumor microenvironment. Breast Cancer Res. 2011;13:213.
17. Witkiewicz AK, Whitaker-Menezes D, Dasgupta A, Philp NJ, Lin Z, Gandara R, et al. Using the "reverse Warburg effect" to identify high-risk breast cancer patients: stromal MCT4 predicts poor clinical outcome in triple-negative breast cancers. Cell Cycle. 2012;11:1108–17.
18. Johnson JM, Cotzia P, Fratamico R, Mikkilineni L, Chen J, Colombo D, et al. MCT1 in invasive ductal carcinoma: monocarboxylate metabolism and aggressive breast cancer. Front Cell Dev Biol. 2017;5:27.
19. Kampf C, Olsson I, Ryberg U, Sjöstedt E, Pontén F. Production of tissue microarrays, immunohistochemistry staining and digitalization within the human protein atlas. J Vis Exp. 2012. https://doi.org/10.3791/3620.
20. Jeong YJ, Jung JW, Cho YY, Park SH, Oh HK, Kang S. Correlation of hypoxia inducible transcription factor in breast cancer and SUVmax of F-18 FDG PET/CT. Nucl Med Rev Cent East Eur. 2017;20:32–8.
21. Lester SC, Bose S, Chen YY, Connolly JL, de Baca ME, Fitzgibbons PL, et al. Members of the Cancer Committee,

College of American Pathologies. Protocol for the examination of specimens from patients with invasive carcinoma of the breast. Arch Pathol Lab Med. 2009;133:1515–38.
22. DeBerardinis RJ, Chandel NS. Fundamentals of cancer metabolism. Sci Adv. 2016;2:e1600200.
23. Danhier P, Banski P, Payen VL, Grasso D, Ippolito L, Sonveaux P, et al. Cancer metabolism in space and time: beyond the Warburg effect. Biochim Biophys Acta Bioenerg. 2017;1858:556–72.
24. Fu Y, Liu S, Yin S, Niu W, Xiong W, Tan M, et al. The reverse Warburg effect is likely to be an Achilles' heel of cancer that can be exploited for cancer therapy. Oncotarget. 2017;8:57813–25.
25. Sotgia F, Whitaker-Menezes D, Martinez-Outschoorn UE, Salem AF, Tsirigos A, Lamb R, et al. Mitochondria "fuel" breast cancer metabolism: fifteen markers of mitochondrial biogenesis label epithelial cancer cells, but are excluded from adjacent stromal cells. Cell Cycle. 2012;11:4390–401.
26. Martinez-Outschoorn UE, Sotgia F, Lisanti MP. Power surge: supporting cells "fuel" cancer cell mitochondria. Cell Metab. 2012;15:4–5.
27. Caro P, Kishan AU, Norberg E, Stanley IA, Chapuy B, Ficarro SB, et al. Metabolic signatures uncover distinct targets in molecular subsets of diffuse large B cell lymphoma. Cancer Cell. 2012;22:547–60.
28. DeNicola GM, Cantley LC. Cancer's fuel choice: new flavors for a picky eater. Mol Cell. 2015;60:514–23.
29. Hensley CT, Faubert B, Yuan Q, Lev-Cohain N, Jin E, Kim J, et al. Metabolic heterogeneity in human lung tumors. Cell. 2016;164:681–94.
30. Sonveaux P, Végran F, Schroeder T, Wergin MC, Verrax J, Rabbani ZN, et al. Targeting lactate-fueled respiration selectively kills hypoxic tumor cells in mice. J Clin Invest. 2008;118:3930–42.
31. Whitaker-Menezes D, Martinez-Outschoorn UE, Lin Z, Ertel A, Flomenberg N, Witkiewicz AK, et al. Evidence for a stromal-epithelial "lactate shuttle" in human tumors: MCT4 is a marker of oxidative stress in cancer-associated fibroblasts. Cell Cycle. 2011;10:1772–83.
32. Doherty JR, Cleveland JL. Targeting lactate metabolism for cancer therapeutics. J Clin Invest. 2013;123:3685–92.
33. Ullah MS, Davies AJ, Halestrap AP. The plasma membrane lactate transporter MCT4, but not MCT1, is up-regulated by hypoxia through a HIF-1alpha-dependent mechanism. J Biol Chem. 2006;281:9030–7.
34. Bovenzi CD, Hamilton J, Tassone P, Johnson J, Cognetti DM, Luginbuhl A, et al. Prognostic indications of elevated MCT4 and CD147 across cancer types: a meta-analysis. Biomed Res Int. 2015;2015:242437.
35. Bellance N, Lestienne P, Rossignol R. Mitochondria: from bioenergetics to the metabolic regulation of carcinogenesis. Front Biosci (Landmark Ed). 2009;14:4015–34.
36. Wurm CA, Neumann D, Lauterbach MA, Harke B, Egner A, Hell SW, et al. Nanoscale distribution of mitochondrial import receptor Tom20 is adjusted to cellular conditions and exhibits an inner-cellular gradient. Proc Natl Acad Sci U S A. 2011;108:13546–51.
37. Ekmekcioglu O, Aliyev A, Yilmaz S, Arslan E, Kaya R, Kocael P, et al. Correlation of 18F-fluorodeoxyglucose uptake with histopathological prognostic factors in breast carcinoma. Nucl Med Commun. 2013;34:1055–67.
38. Ueda S, Tsuda H, Asakawa H, Shigekawa T, Fukatsu K, Kondo N, et al. Clinicopathological and prognostic relevance of uptake level using 18F-fluorodeoxyglucose positron emission tomography/computed tomography fusion imaging (18F-FDG PET/CT) in primary breast cancer. Jpn J Clin Oncol. 2008;38:250–8.
39. García Vicente AM, Soriano Castrejón A, León Martín A, Chacón López-Muñiz I, Muñoz Madero V, Muñoz Sánchez Mdel M, et al. Molecular subtypes of breast cancer: metabolic correlation with ^{18}F-FDG PET/CT. Eur J Nucl Med Mol Imaging. 2013;40:1304–11.
40. Kadoya T, Aogi K, Kiyoto S, Masumoto N, Sugawara Y, Okada M. Role of maximum standardized uptake value in fluorodeoxyglucose positron emission tomography/computed tomography predicts malignancy grade and prognosis of operable breast cancer: a multi-institute study. Breast Cancer Res Treat. 2013;141:269–75.
41. Aogi K, Kadoya T, Sugawara Y, Kiyoto S, Shigematsu H, Masumoto N, et al. Utility of ^{18}F FDG-PET/CT for predicting prognosis of luminal-type breast cancer. Breast Cancer Res Treat. 2015;150:209–17.
42. García Vicente AM, Soriano Castrejón A, López-Fidalgo JF, Amo-Salas M, Muñoz Sanchez Mdel M, Álvarez Cabellos R, et al. Basal ^{18}F-fluoro-2-deoxy-D-glucose positron emission tomography/computed tomography as a prognostic biomarker in patients with locally advanced breast cancer. Eur J Nucl Med Mol Imaging. 2015;42:1804–13.
43. Groheux D, Giacchetti S, Delord M, de Roquancourt A, Merlet P, Hamy AS, et al. Prognostic impact of 18F-FDG PET/CT staging and of pathological response to neoadjuvant chemotherapy in triple-negative breast cancer. Eur J Nucl Med Mol Imaging. 2015;42:377–85.
44. Porporato PE, Filigheddu N, Pedro JMB, Kroemer G, Galluzzi L. Mitochondrial metabolism and cancer. Cell Res. 2018;28:265–80.